Diamond Turned, Light Weight, Athermal, Visible TMA Telescope for the Planned New Horizons Mission to Pluto

M.J. Hegge, J.W. Baer, L.M.R. Hardaway, G. Taudien, D.S. Sabatke, S.R. Shidemantle
Ball Aerospace & Technologies Corp
1600 Commerce Street
Boulder, Colorado, USA 80306

J.J. Santman, L.E. Comstock
Corning NetOptix - Diamond Turning Division
69T Island Street
Keene, New Hampshire, USA 03431

ABSTRACT

Unpolished diamond turned mirrors are common for infrared systems. We report the successful use of unpolished mirrors in a visible spectrum, all aluminum telescope for the planned New Horizons mission to Pluto. The Ralph telescope is an F/8.7 Three Mirror Anastigmat with a 75mm aperture, a 5.7º by 1.0º field of view, and a mass of only 8kg. Key to the performance of the system are a process for reducing the micro-roughness of the off-axis aspheric surfaces to below 60 Ångstroms RMS, and the fabrication of precision diamond turned mounting features on the mirrors and one-piece, thin-walled housing. The telescope achieves nearly diffraction-limited performance with minimal post-assembly alignment, and maintains that performance, including focus, over a wide range about the operating temperature of 210K.

1. BACKGROUND

The planned New Horizons Mission to Pluto, its large satellite Charon, and the Kuiper Belt, is a NASA New Frontiers project.[1] A key mission goal is getting to Pluto at ~32 AU from the sun, before its atmosphere freezes onto the surface as it moves farther from the sun in its orbit, and while it is still close to its equinox, so that neither pole is in perpetual darkness. This dictates a fast flight, and requires the largest launcher and a small spacecraft. Lightweight and low power instruments are mandatory. The Ralph instrument must also operate at reduced temperatures to enable the recording of infrared spectra with the Linear Etalon Imaging Spectrometer Array (LEISA) detector, and needs a very wide field of view to map the entire planet with its Multispectral Visible Imaging Camera (MVIC) TDI arrays. Sitting on the outside of the spacecraft, the operating temperature range is 195K to 225K and the survival temperature is 150K.The requirement for a gravity assist at Jupiter dictates a launch in January of 2006, which resulted in a very compressed schedule. The design of the Ralph instrument optics was critical in meeting each of these requirements.

2. TECHNICAL DESCRIPTION

The Ralph telescope is an F/8.7 Three Mirror Anastigmat with an unobstructed 75 mm aperture, and a 5.7º by 1.0º field of view. Its three mirrors are uncoated, diamond-turned, aluminum optics (ellipse-convex hyperbola-ellipse) with parallel optical axes. These optics are mounted in a one-piece, thin-walled Aluminum optical housing. The optics are fabricated with integral precision mounting features and mount to the exterior of the housing using precision pins, which facilitate “bolt-and-go” assembly. Post assembly alignment consisted solely of translation of the Primary mirror. All of the mounting pads are parallel, and the mounting pads for the Primary and Tertiary mirrors are in a single plane, as seen on the right in Figure 3. This greatly facilitates fabrication, as the pads were diamond flycut in a single operation. A beamsplitter is used to split the optical beam to two detector assemblies. Figure 1 shows the Code-V diagram of the Ralph optical train.

Optomechanics 2005, edited by Alson E. Hatheway, Proceedings of SPIE Vol. 5877 (SPIE, Bellingham, WA, 2005)
0277-786X/05/$15 · doi: 10.1117/12.617018

Downloaded From: http://proceedings.spiedigitallibrary.org/ on 05/24/2013 Terms of Use: http://spiedl.org/terms

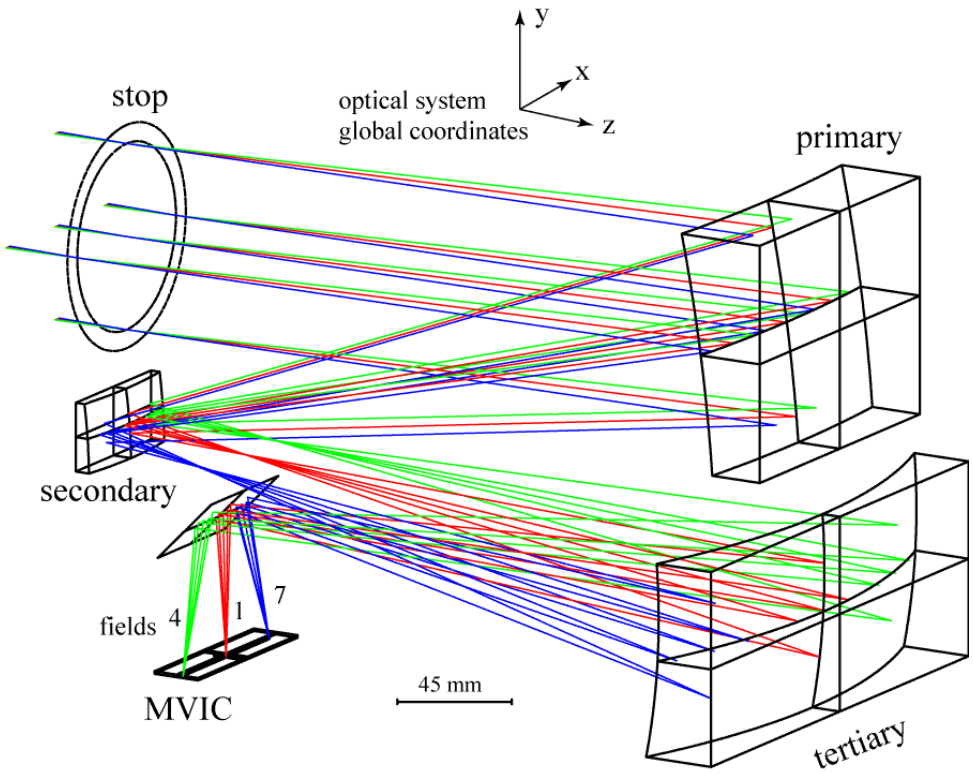

Figure 1. Ralph Optical Train

The housing is approximately 300 mm long, 200 mm wide and 170 mm tall. Figure 2 shows the CAD model of the optical housing, optics, and detector assemblies.

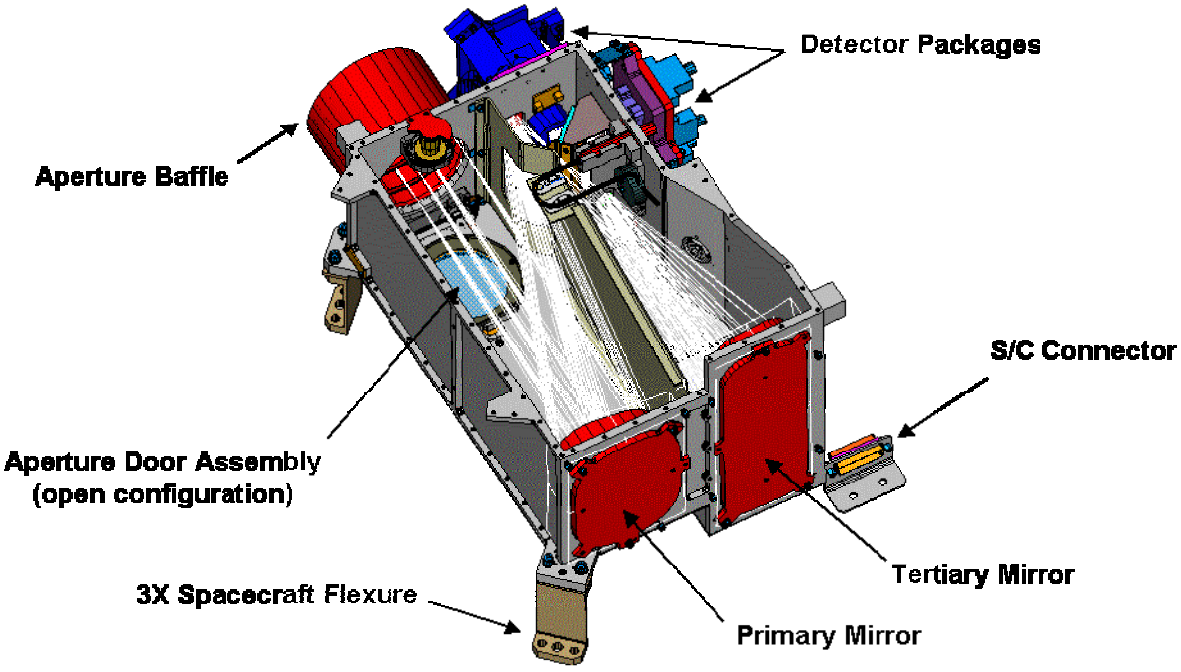

Figure 2. Ralph CAD Model

Downloaded From: http://proceedings.spiedigitallibrary.org/ on 05/24/2013 Terms of Use: http://spiedl.org/terms

The system wavefront error was specified to be less than 0.15 waves RMS at 633nm. The mirrors were require to have surface figure errors less than 0.1 waves P-V at 633nm and surface roughness <60 Angstroms RMS.

The Aluminum housing is made from a single billet of 6061-T651 Aluminum with its grain running parallel to the long dimension. A large rectangular piece was removed from the middle of the billet using wire EDM, followed by extensive machining of the outside. Reverse thermal quenching was used to stabilize the material before and after rough machining. After final machining the part was black anodized (Type III). Figure 3 shows the Ralph Optical Housing after machining.

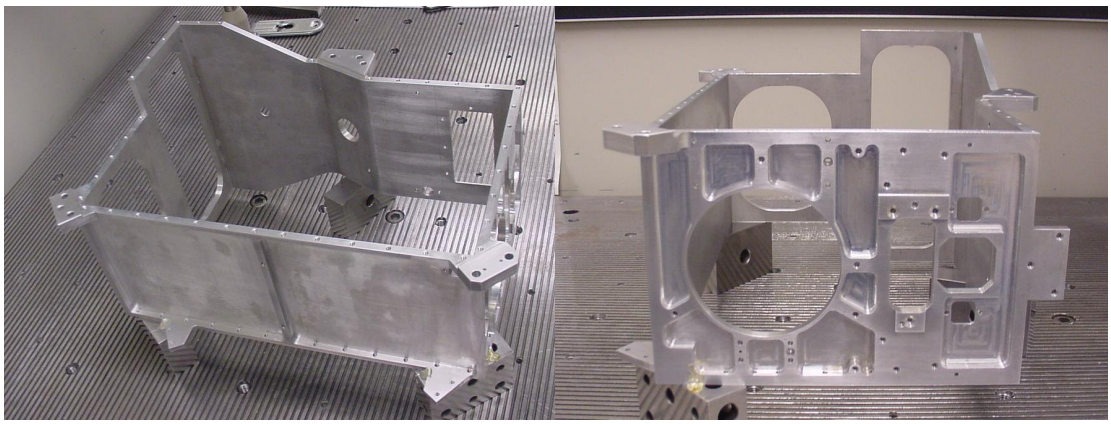

Figure 3. Ralph Optical Housing

Once complete, the top and bottom covers were assembled on the housing. The optical pads of the housing were diamond turned to accept the Ralph mirrors. The housing was then disassembled for cleaning. Upon reassembly, the optical performance did not meet the requirements. It was determined that the covers, visible in Figure 4, were distorting the housing. Because the corner covers were not pinned or otherwise mechanically registered, variations in the reassembly sequence resulted in a strained housing, as evidenced by abrasions left on the perimeter of fastener clearance holes. One of these corner covers is visible in the left half of Figure 4 as the gold colored element in the upper right.

To ensure a stable telescope assembly, the top cover was split into two parts. The larger part with the corner caps became permanent and the other was removable, and can be seen on the left in Figure 4. The bottom cover, corner cap, and a long central baffle were installed permanently as well, which contributed to the stiffness of the box. The removable cover was installed using a well-defined torque sequence. In this configuration, the box was cleaned and bagged with the optic mounting pads exposed. The optics pads were then diamond turned again. The result was a housing that easily met the mirror parallelism specification.

Once the optics were installed and aligned the optic interface pins were bonded. Figure 4 shows this configuration.

Downloaded From: http://proceedings.spiedigitallibrary.org/ on 05/24/2013 Terms of Use: http://spiedl.org/terms

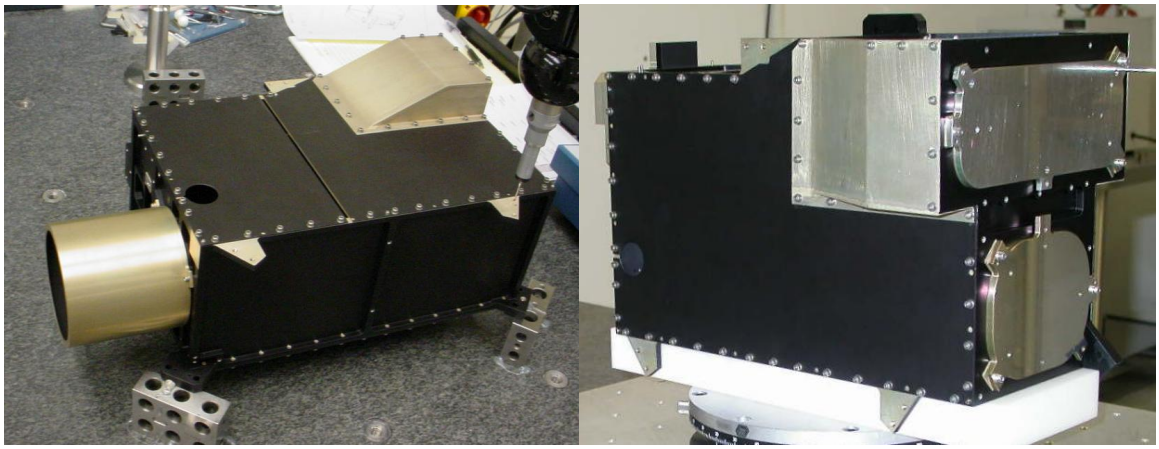

Figure 4. Ralph Telescope Assembly

3. SURFACE ROUGHNESS REDUCTION

For years, single-point diamond turning has been associated with producing mirrors that are typically more suitable for infrared applications. Aluminum is typically the material of choice for diamond turned mirrors because of its relatively low cost, structural and thermal stability, and its compatibility with the turning process, but the diffractive effects of the diamond turning "grooves" were generally too severe to provide adequate performance in the visible and UV spectral ranges.

The Ralph mirrors were fabricated by Corning NetOptix - Diamond Turning Division using their proprietary "LEC" process, which dramatically reduces the diffraction effects of diamond turned aluminum mirrors. By achieving low roughness in the diamond turning, this process obviates the use of conventional polishing, which is expensive and inevitably results in some loss of registration of the optical surfaces to the mechanical features of the parts.

Figure 5a,shows roughness and a surface map of a 1mm section of a traditionally diamond machined, 6061 Aluminum substrate mirror using data measured with a WYKO NT2000 non-contact profilometer. Diamond tooling marks are prominent in the image, which show as parallel streaks.

Figure 5b shows a section of an identical mirror manufactured with the LEC process. The RMS surface roughness is about half of that of the standard process. Equally important, the parallel tooling marks have been dramatically reduced. The particulate matter inherent in the alloy, the "grain" of the material, is now the most prominent contributor to surface roughness and therefore to scattered light.

Downloaded From: http://proceedings.spiedigitallibrary.org/ on 05/24/2013 Terms of Use: http://spiedl.org/terms

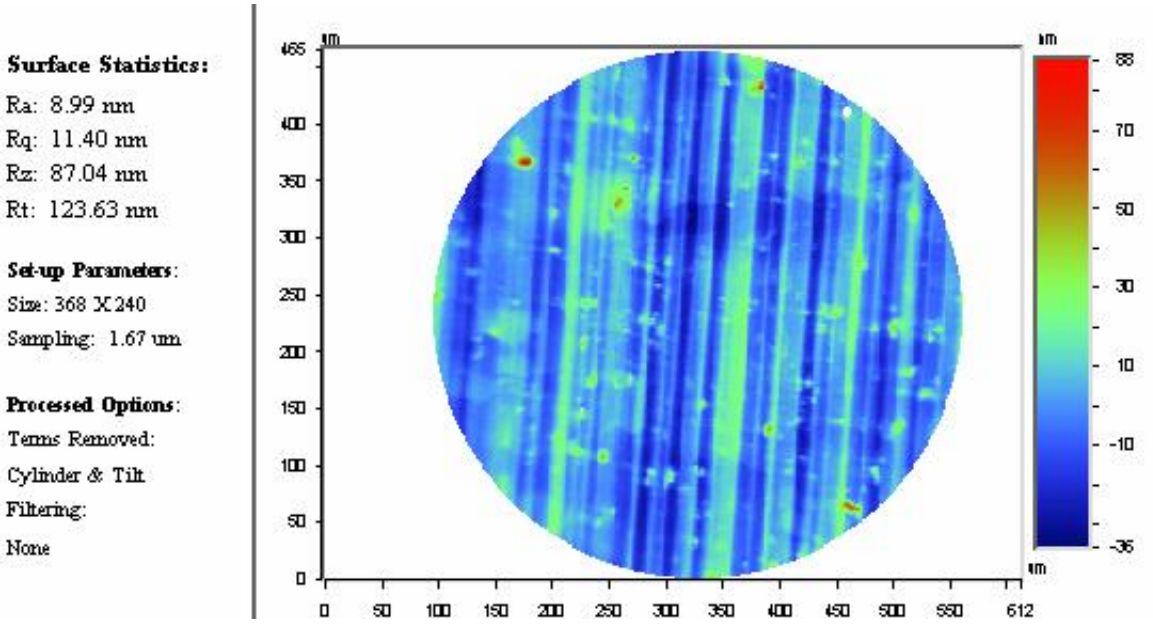

Figure 5a. Traditional Diamond Turned Aluminum Optic

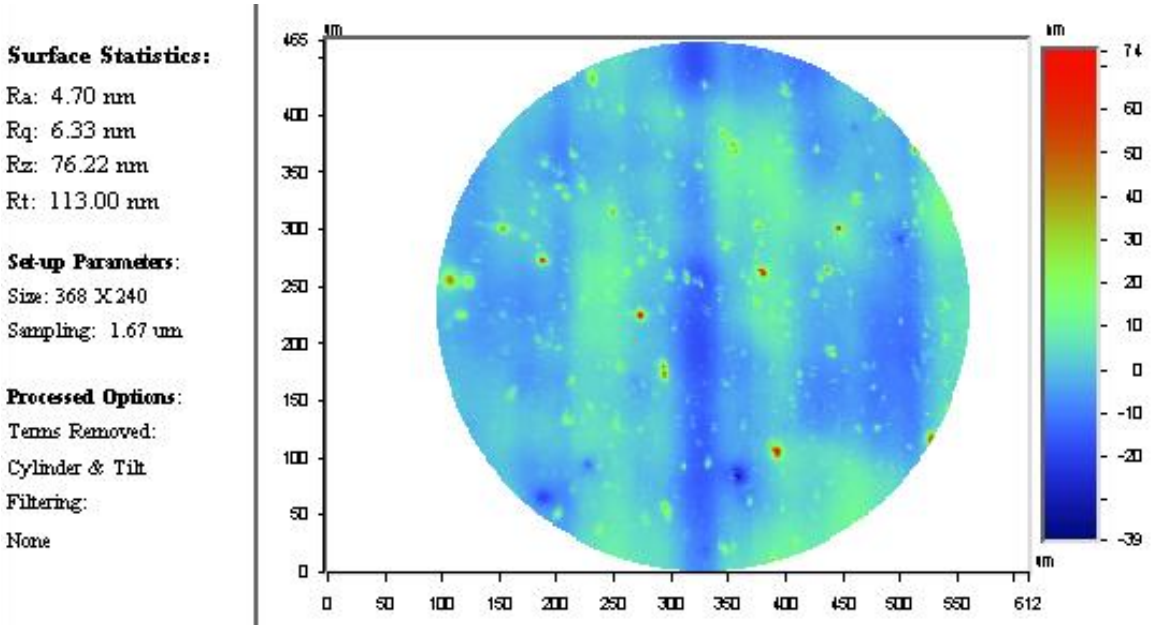

Figure 5b. Diamond Turned Aluminum Optic Using the LEC Process

The improvement in surface quality can be quantified by measuring the surface Power Spectral Density (PSD) and BRDF, which are generally accepted measurement standards for quantifying roughness of optical surfaces,[2]. Figure 6 shows PSD measurements for both a traditionally diamond machined 6061 Aluminum mirror, and for a LEC-processed mirror with an identical substrate. Note that in the Y-axis, measurements are quite similar, because the observation axis runs parallel to the diamond turning "grooves. However, along the X-axis, perpendicular to the tooling marks, the PSD of the conventionally-turned mirror is significantly degraded. The LEC mirror shows a much lower PSD. Moreover, the PSD curve is very smooth with relatively few "spikes" and greatly reduced "diffractive grating" effects.

Downloaded From: http://proceedings.spiedigitallibrary.org/ on 05/24/2013 Terms of Use: http://spiedl.org/terms

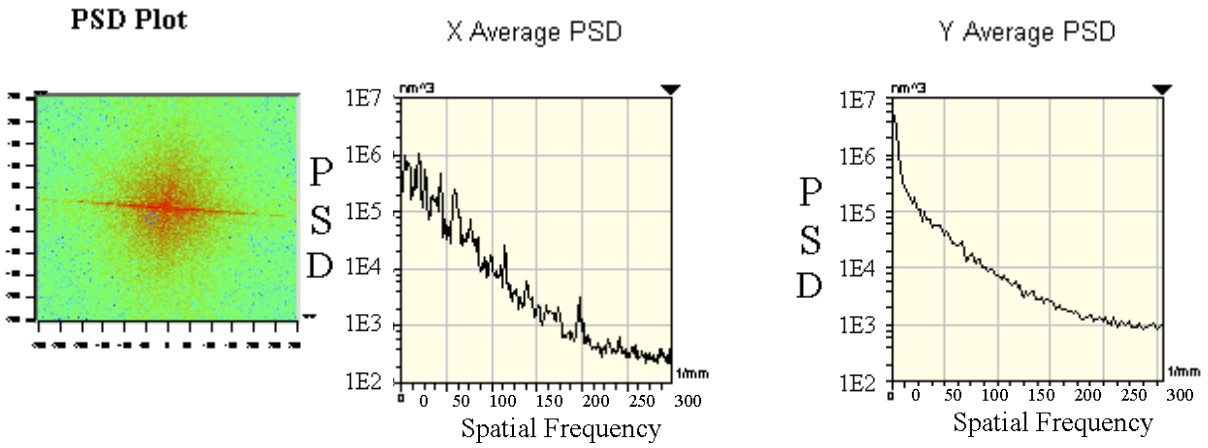

Figure 6a. PSD of a Traditionally Diamond Turned Aluminum Optic

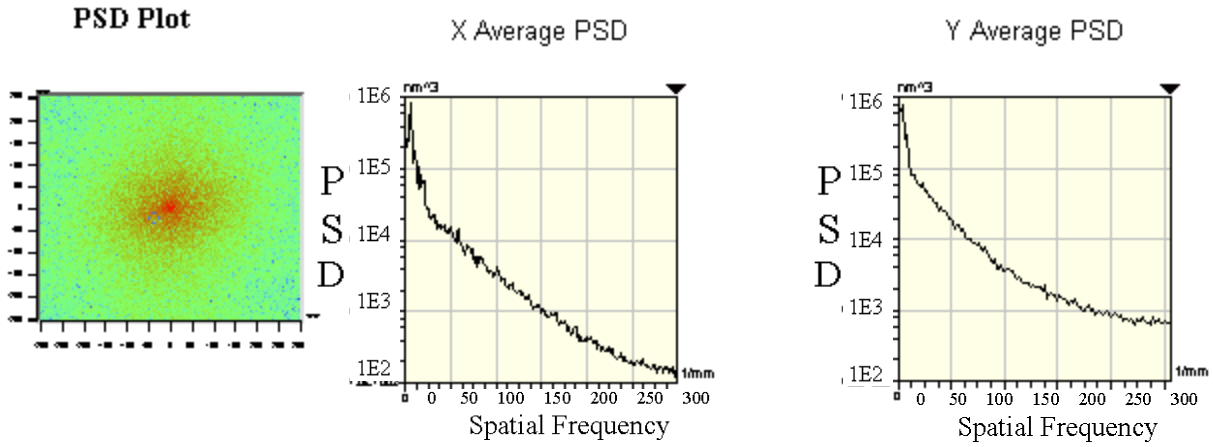

Figure 6b. PSD of a Diamond Turned Optic Using the LEC Process

The result of this difference between the two mirrors can be seen in the PSD plots. The horizontal spikes in the plot for the traditionally diamond turned mirror are numerous "satellite" spots created by the diamond tooling marks, which essentially act as a random grating. This feature is largely absent for the LEC mirror. This can also be seen in the lack of structure in the X-axis PSD plot. The measured surface roughness of the each flight mirror is included with the mirror data in Table 1.

Mirror	Primary	Secondary	Tertiary
Size (mm)	117 x 92	54 x 26	190 x 75
Roughness (Å RMS)	56	49	76
Surface Figure Error (λ RMS @ 633nm)	0.032	0.056	0.075
Surface Figure Error (λ PV @ 633nm)	0.193	0.264	0.494

Table 1. Mirror Parameters

4. FLING

Production planning originally called for a rotation rate greater than 500 RPM during diamond turning of the mirrors. A number of factors must be considered in setting this parameter, including surface finish, production time and surface deformation from centrifugal forces. The latter effect, referred to as *fling*, is significant to high quality optical systems, even with solid mirrors. Solid mirrors provided the lowest risk

Downloaded From: http://proceedings.spiedigitallibrary.org/ on 05/24/2013 Terms of Use: http://spiedl.org/terms

solution by trading an acceptable mass increase for reduced modeling complexity, and eliminating the time that would have been involved in iterating the design and analysis of lightweigting features.

Fling causes the mirror substrate to deform during turning, while the presumably correct radial profile is applied by the diamond-tipped tool. With the cessation of centrifugal forces when the lathe is stopped, the surface rebounds leaving a net error opposite in sign to the original deformation.

Structural and optical modeling was performed to assess the impact of fling on the Ralph system. The small size and off-axis distance of the secondary mirror made it relatively impervious to fling, so only the primary and tertiary were included in the analysis. Their deformations during turning were predicted using finite element models and a static analysis in MSC NASTRAN (Figure 7). Linear constraints were employed to model mounting screws and pins joining the mirror substrates to the rigid lathe fixture. Other nodes at the mirror/fixture interface were constrained as necessary to prevent them from sagging into the fixture. This was a simple measure to avoid the increased computation required by a non-linear model for the interface.

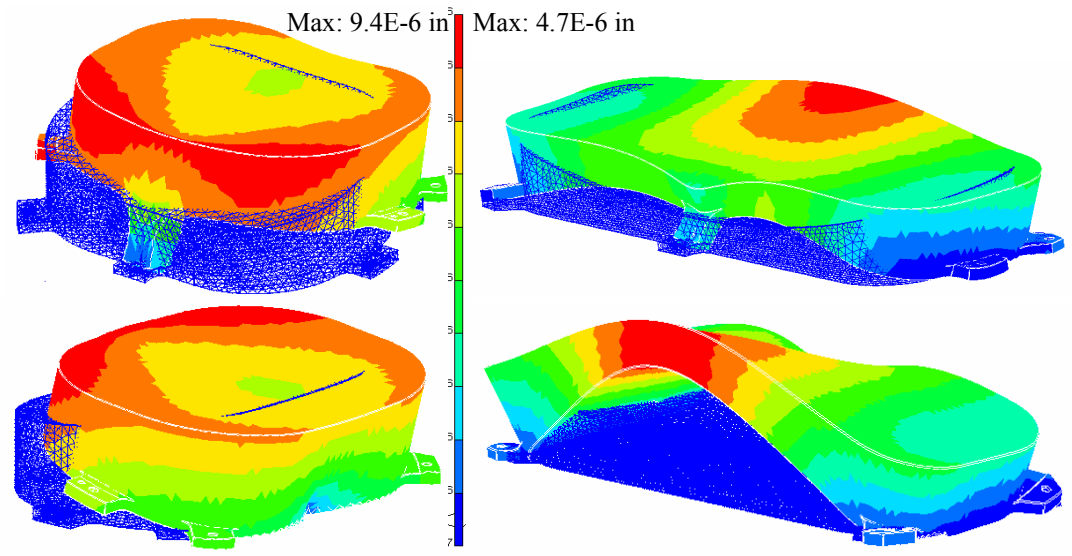

Figure 7. Finite element models for the primary (left) and tertiary mirrors. The predicted deformations (overlaid) are shown greatly exaggerated.

In the optical portion of the analysis, the predicted deformations were inverted to account for rebound. A best-fit radial function, centered on the lathe axis, was subtracted from the resulting surface figure error (SFE) data to model compensation applied during diamond turning based on measured interferograms. The results are shown in Figure 8, with beam footprints for three field points chosen for analysis outlined in white.

Downloaded From: http://proceedings.spiedigitallibrary.org/ on 05/24/2013 Terms of Use: http://spiedl.org/terms

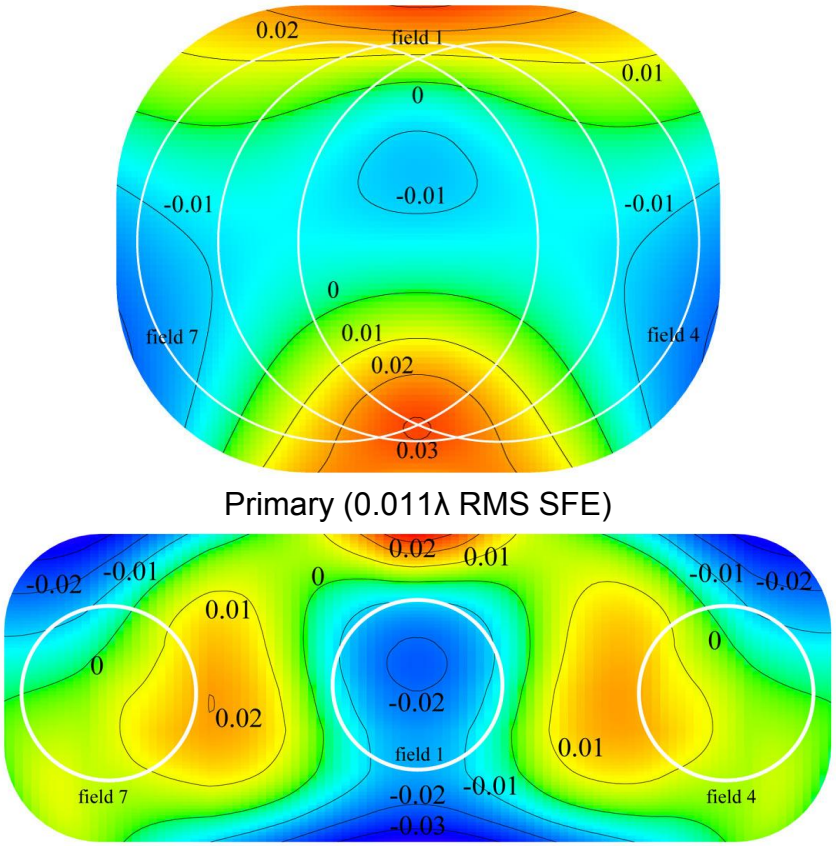

Figure 8: Predicted SFE in waves at 632.8 nm over the full clear aperture of each mirror. Best-fit piston, tip, tilt and defocus have been subtracted. The beam footprints are shown outlined in white.

For a given field point; only the surface figure errors within the corresponding beam footprint contribute to the system wavefront error. After extracting data within footprints, accounting for beam inversion, and subtracting mean defocus and astigmatism[3] (which can be compensated in alignment) system RMS wavefront errors of about 0.004 waves were predicted. These were negligible in comparison to other error terms.

Despite the favorable predictions of the analysis, measured surface figure errors for preliminary diamond tool passes with a 500 RPM rotation rate showed considerably larger errors. Possible culprits include the absence of non-linear constraints in our model of the substrate/fixture interface, and forces applied by the diamond-point tool, which were neglected in our analysis. The rotation rate was reduced to less than 400 RPM (>36% reduction in centrifugal forces), which yielded acceptable results.

5. SYSTEM PERFORMANCE

Upon assembly, the optical performance was <0.16 waves RMS wavefront error across the 5.7º wide Field of View before any alignment ("bolt and go"). Alignment consisted solely of translating the Primary mirror. Although the 0.015" radial clearance on the pins was inadequate to reach the point of ideal alignment, at the limit of motion the average WFE for seven fields across the FOV was 0.075 waves RMS, essentially diffraction limited. Figure 9 shows two pass system interferograms for the on-axis and edge-of-field, worst-case performance field points. This testing was repeated at 200K, where the system was seen to maintain its performance.

Downloaded From: http://proceedings.spiedigitallibrary.org/ on 05/24/2013 Terms of Use: http://spiedl.org/terms

Position A	On Axis
Wavelength	633nm
RMS WFE	0.044 λ
20 pt PV	0.333 λ
Removed	Tilt, Power
Data Points	128630

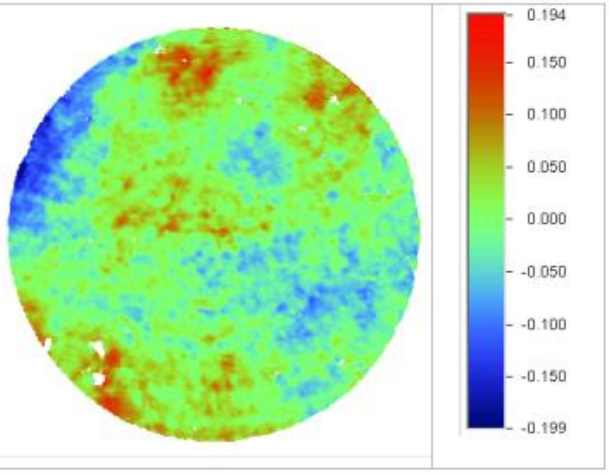

Position C	Field Edge
Wavelength	633nm
RMS WFE	0.101 λ
20 pt PV	0.643 λ
Removed	Tilt, Power
Data Points	127797

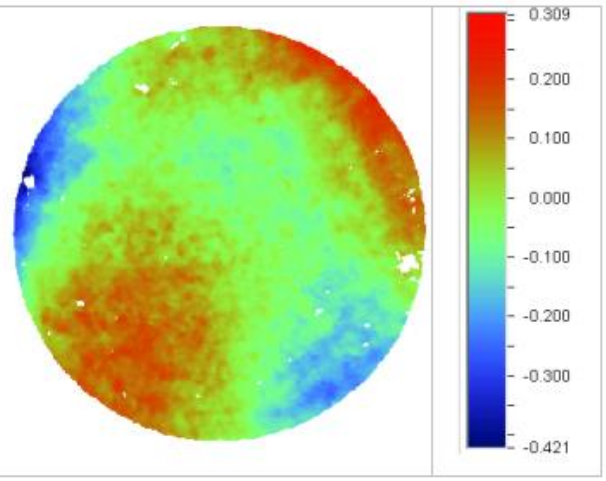

Figure 9. Interferograms and data for two selected field locations (The wavefront errors include contributions from precision ball bearings used as return spheres.)

6. CONCLUSION

The Ralph Instrument, which includes the telescope, was successfully tested and delivered for integration onto the New Horizons spacecraft in March of 2005. The telescope exceeds all optical requirements and has remained stable throughout integration and testing.

7. REFERENCES

1. A. S. Stern and J. Spencer, New Horizons: The First Reconnaissance Mission to Bodies in the Kuiper Belt, Earth, Moon, and Planets, v. 92, p. 477-482 (2003).
2. J. C. Stover, "Optical Scattering Measurement and Analysis," 2nd ed. SPIE Press, Bellingham, WA (1995).
3. J. C. Wyant and K. Creath, "Basic Wavefront Aberration Theory for Optical Metrology", in R. Kingslake, ed., *Applied Optics and Optical Engineering*, vol. XI. New York: Academic, 1992.

Downloaded From: http://proceedings.spiedigitallibrary.org/ on 05/24/2013 Terms of Use: http://spiedl.org/terms